

The ATHAS database on heat capacities of polymers

Bernhard Wunderlich

*Department of Chemistry, The University of Tennessee, Knoxville, TN 37996-1600, and
Chemical and Analytical Sciences Division, Oak Ridge National Laboratory,
Oak Ridge, TN 37831-6197, USA*

Abstract: Data of thermodynamic properties of polymers have in the past been neglected by main-stream collections. The well-founded reason for this is the common non-existence of equilibrium in polymeric materials. In the meantime, however, extrapolation methods and special polymerization and crystallization techniques have been developed to assess the equilibrium properties of polymers. The *ATHAS* data bank, for example, contains such equilibrium information on heat capacities from 0 to 1000 K, vibrational spectra, transition parameters, enthalpies, free enthalpies, and entropies for over 200 polymers and polymer-related materials. The availability of such data for polymers proved of great importance for the analysis of metastable states. With reference to the equilibrium limit, stability estimates can be made and detailed studies are possible of the superheating on melting and supercooling on crystallization. Comparisons of the vibrational heat capacities with measured data reveal conformational motion in polymers. A new mesophase, that of condensation crystals, could be defined. A new glassy state, the rigid amorphous state, could be identified. For the first time, it became even possible to analyze drawn fibers using a multi-phase approach based on thermal and structural analyses.

INTRODUCTION

Flexible linear macromolecules, usually simply called polymers, owe their special place among materials to their overriding importance of conformational motion and disorder. The basis of the understanding of polymers was developed between 1920 and about 1950. The *Advanced Thermal Analysis System*, *ATHAS*, had its start in 1975, but work in thermal analysis by the author, initially under the direction of Professor Malcolm Dole, dates back to 1955 [1]. At that time the total scientific literature on heat capacities of linear macromolecules was no more than perhaps 10–20 publications. We observed early that the problem of thermal analysis of linear macromolecules rested with metastable and unstable samples. It was necessary to convert the slow, adiabatic calorimetry to fast scanning techniques [2] that permitted the evaluation of the thermodynamic properties under zero-entropy-production conditions, *i.e.* conditions that allow analysis without change in stability of the system [3]. Into this time period falls also the first detailed interpretation of the heat capacity of polyethylene [4]. A first review of the topic [5] coupled with initial attempts at empirical addition schemes [6] rounded out the early work on thermal analysis of macromolecules.

This first effort was followed by an extensive study of nonequilibrium melting and glass transitions. Work on melting transitions led to the discovery of superheating and the development of various techniques to analyze nonequilibrium crystals, summarized in Ref. [7]. The glass transition effort centered about a rule of constant increase of heat capacity at the glass transition temperature [8], a study of the hysteresis phenomena [9], and the effect of pressure on vitrification [10].

By 1975 it became increasingly obvious that a major effort in combining all knowledge and data on the thermal analysis of linear macromolecules could bring considerable progress to the field. The first summaries of *ATHAS* are given in Refs. [11]. The *ATHAS* effort led first to the establishment of a critically reviewed data bank of experimental heat capacities [12]. Based on the knowledge drawn from this data bank, a rigid amorphous state was discovered in semicrystalline and drawn macromolecules [13], and conformationally disordered states (condensation states) could be identified

as a new type of phase [14]. Much of the text and many of the figures for this review are based on the Textbook "Thermal Analysis," that summarizes the present state [15].

Experimental Heat Capacities of Crystalline and Amorphous Polymers

Linear macromolecules do not normally crystallize completely, they are semicrystalline, and thus present a nonequilibrium system. Kinetic and structural reasons cause the partial crystallization. The two main kinetic restrictions are incomplete transfer of the randomly coiled and entangled molecules to the crystal, and incomplete extension to the equilibrium, extended-chain macroconformation once the molecules are in the crystal (chain-folding principle) [7]. The structural reasons for the hindrance of crystallization lie in irregularities within the molecular chains. Copolymers and stereoirregular polymers may, for example, remain amorphous at all temperatures.

The first step in the analysis of the thermal properties of linear macromolecules must be to establish the crystallinity dependence of the heat capacity. Polyethylene, the most analyzed polymer [12], is treated as an example. The fact that polyethylene, $(\text{CH}_2-)_x$, is semicrystalline implies by itself that the sample is metastable, *i.e.* not in equilibrium. Thermodynamics requires that a one-component system like polyethylene can have a two-phase equilibrium only at the melting temperature (phase rule [15]). The weight fraction crystallinity, w_c , can be established from density measurements (dilatometry):

$$w_c = (\rho_c/\rho)[(\rho_c - \rho_a)/(\rho - \rho_a)] \quad (1)$$

where ρ is the density in Mg/m^3 , subscript c designates the completely crystalline state (determined, for example, by X-ray crystal-structure-analysis), and subscript a, the amorphous state (glassy or liquid). Plotting the measured heat capacities of samples with different crystallinity results often in linear relationships. Such plots allow the extrapolation to crystallinity zero and 1.0 to find the heat capacities of the amorphous and crystalline states, respectively, even if these limiting states are not experimentally accessible.

Figure 1 illustrates in its left graph the experimental heat capacities for polyethylene at very low temperatures. The crystallinity dependence of the heat capacity for a number of other polymers is described in the *ATHAS* data bank of experimental heat capacities [12]. For the fully crystalline polyethylene ($w_c = 1.0$) there is a T^3 temperature dependence of the heat capacity up to about 10 K (single point in the graph). Such T^3 temperature dependence is required for the low-temperature limit of a three-dimensional Debye function [16] that describes heat capacities of solids. It is caused by a quadratic increase in number of vibrators with increasing frequency, ν . The amorphous polyethylene ($w_c = 0$) seems, in contrast, never to reach a T^3 temperature dependence of the heat capacity. The curves of the figure do not even change monotonously with temperature.

As the temperature is raised, the crystallinity dependence of the heat capacity becomes less, and is only a few percent between 50 to 200 K. In this temperature range the heat capacity is largely independent of the physical structure. Glass and crystal have almost the same heat capacity. This is followed, again, by a steeper increase in heat capacity as the amorphous polymer undergoes its glass transition at about 230–250 K. The bottom lines in the right graph of Fig.1 show the crystallinity dependence in the glass transition region. It is of interest to note that the fully amorphous heat capacity at 260 K from this graph agrees well with the extrapolation of the heat capacity of the liquid from above the melting temperature (414.6 K).

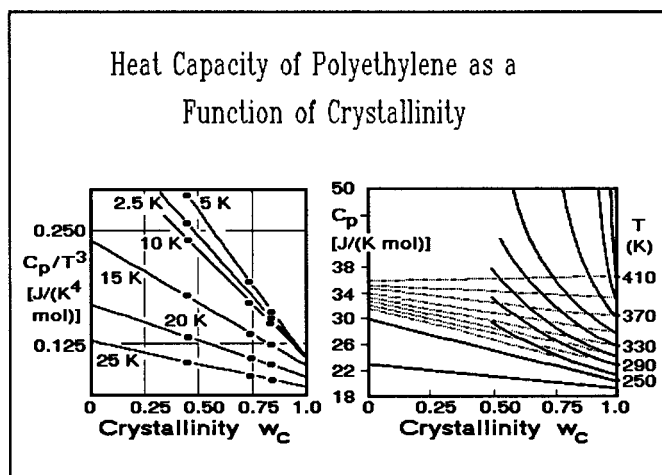


FIGURE 1

Extrapolated Heat Capacities of Polyethylene to the Fully Amorphous and the Fully Crystalline States

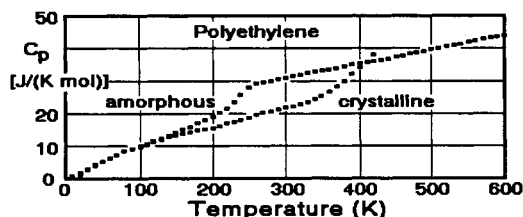


FIGURE 2

ments and extrapolations. The latent heat (heat of fusion) is extrapolated to crystallinity 1.0 and the equilibrium melting temperature and added to the enthalpy of thermal motion ($H - H_c^\circ = \int C_p dT$). Entropy ($S = \int C_p/T dT$) and Gibbs function (free enthalpy, $G = H - TS$) can similarly be determined and for the ATHAS data bank in form of tables and graphs, as shown in Fig. 3.

Interpretation of the Heat Capacity

An important aspect of the ATHAS data bank is a theoretical or empirical interpretation of the critically reviewed experimental data whenever possible. The T^3 -dependence of C_p of crystalline polyethylene in Fig. 2, for example, indicates that in the limited temperature range between 0 and 10 K the three-dimensional Debye model holds. It links heat capacity to a vibrational spectrum, as will be shown below [Eq. (8)]. Next, there is a change to a linear temperature dependence of C_p of both, crystalline and amorphous solids that continues to about 200 K. Such temperature dependency fits a one-dimensional Debye function that is based on a constant number of vibrators over a range of frequencies going from 0 to θ_1 [16,17], with θ_1 representing a characteristic frequency expressed in temperature ($1 \text{ Hz} = 4.80 \times 10^{-11} \text{ K}$, $1 \text{ cm}^{-1} = 1.44 \text{ K}$):

$$C_v/3N = D_1(\theta/T_1) \quad (2)$$

$$D_1(\theta/T_1) = (T/\theta_1) \int_0^{\theta/T_1} \{(\theta/T)^2 \exp(\theta/T) / [\exp(\theta/T) - 1]^2\} d(\theta/T) \quad (3)$$

$$\theta = hv/k \quad (4)$$

Between 200 and 250 K one notices a slowing of the increase of the crystalline heat capacity with temperature, to show a renewed increase above 300 K, to reach close to the melting temperature values equal to and higher than the heat capacity of liquid polyethylene.

The heat capacity of the glassy polyethylene shows large deviations from the heat capacity of the crystal at low temperature. At these temperatures, the absolute value of the heat capacity is so small that it does not show up in Fig. 2. The reason for the deviation from a three-dimensional Debye function, seen in Fig. 1, is not well understood. After a long temperature range of close to equal heat capacities of crystal and glass, the glass transition is obvious at 237 K. A small increase

Above about 260 K, melting of small, metastable crystals causes the abnormal, nonlinear deviations in the heat capacity vs. crystallinity plot. The measured data are indicated by the heavy lines in the figure. The thin, broken lines indicate how continued additivity without melting would look. All contributions above the broken lines must, thus, be assigned to the nonequilibrium melting and excluded from the data bank heat capacities.

The results of the extrapolations of Fig. 1 are shown in Fig. 2. The glass transition is obvious in curve for the amorphous heat capacity (237 K), the equilibrium melting point is known to be 416.6 K from separate measure-

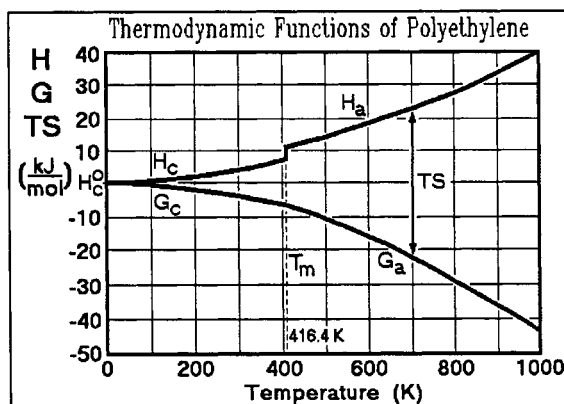


FIGURE 3

in the amorphous heat capacity beyond the values of the crystals starts already at about 110 K and has been linked to the γ -transition that is caused by a local conformational motion [4]. In the liquid state, the heat capacity is linear over a very wide temperature region. Only first efforts have been made to develop a detailed description of the motion in the liquid state [18].

This quite complicated temperature dependence of the solid heat capacity is to be linked next to a more detailed, approximate microscopic model of thermal motion. The basic equations linking vibrational frequencies to heat capacity are the Einstein function [19,20]:

$$C_v/N = E(\Theta/T) \quad (5)$$

$$E(\Theta/T) = [(\Theta/T)^2 \exp(\Theta/T)] / [\exp(\Theta/T) - 1]^2 \quad (6)$$

and the Debye functions [16,17,21,22] of which the one-dimensional one was given as Eq. (3) and the three-dimensional one is:

$$C_v/3N = D_3(\Theta/T_1) \quad (7)$$

$$D_3(\Theta/T_3) = 3(T/\Theta_3)^3 \int_0^{\Theta/T_3} \{[(\Theta/T)^4 \exp(\Theta/T)] / [\exp(\Theta/T) - 1]^2\} d(\Theta/T) \quad (8)$$

As an initial try, one can invert the vibrational spectrum of crystalline polyethylene, known in some detail from normal mode calculations using force constants derived from infrared and Raman spectroscopy [23]. Using a different Einstein function for each normal mode vibration [Eq. (6)], one can compute a heat capacity. The heat capacity of the crystalline polyethylene shown in Fig. 2 can be reproduced in this way, but only above about 50 K. Below 50 K the experimental data show increasing deviations, an indication that the computation of the low-frequency skeletal vibrations cannot be carried out with sufficient precision [24]. To overcome the error in C_p when computed from the low vibration frequencies, a method of generating approximate spectra was developed.

Calculation of Heat Capacity of Solid Polymers from an Approximate Frequency Spectrum

For polyethylene and most other polymers one can distinguish between skeletal and group vibrations. The first reach from 0 to approximately 2×10^{13} Hz. Polyethylene shows two degrees of freedom (N) in this frequency range. The motion involved in these vibrations can be visualized as torsional and accordion-like motions of the CH_2 -backbone, as illustrated in sketches 1 and 2 of Fig. 4. The torsion involves mainly bond rotation, the accordion-like motion bending of the C-C-C-bonds. Their frequencies are such that they contribute mainly to the increase in heat capacity from 0 to 200 K.

The group vibrations occur at a somewhat higher frequency. This gap in the frequency distribution is responsible for the levelling of the heat capacity between 200 and 250 K (see Fig. 2). In the plateau region C_p is of the proper order of magnitude for the assumed two degrees of freedom (*i.e.* about 16–17 J/(K mol) or $2R$).

The group vibrations originate from the relatively isolated groupings of atoms along the backbone chain. In

the first set of group vibrations, between 2 and 5×10^{13} Hz, there are five degrees of freedom, involving mainly C-H-bending and C-C-stretching motions. The sketches 3–6 in Fig. 4 illustrate the approximate C-H-motions of the bending vibrations. The stretching vibration of the C-C-bond [sketch (9)] falls into the same frequency range as the C-H-bending. Due to the close to 90° bond angle (110°), the C-C-stretching is not coupled sufficiently along the chain to result in a skeletal vibration of broad frequency distribution. These latter five vibrations are responsible for the renewed

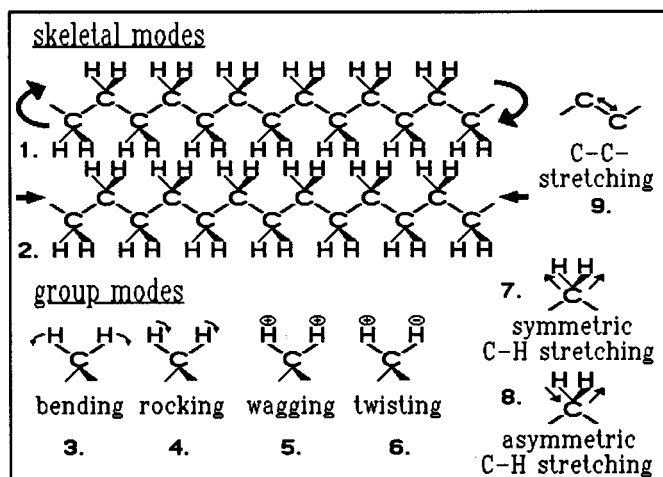


FIGURE 4

increase of the heat capacity in Fig. 2 starting at about 300 K. Below 200 K their contributions to the heat capacity are small.

Finally, the CH₂-groups have two more group vibrations of very high frequencies, above 8×10¹³ Hz. These are the C-H-stretching vibrations, given by the bottom sketches (7) and (8) of Fig. 4. These frequencies are so high, that at 400 K their contribution to the heat capacity is still small. The total of nine vibrations possible for the three atoms of the CH₂-unit would, when fully excited, lead to a heat capacity of 75 J/(K mol). At the melting temperature, only half of these vibrations are excited, C_v is about 38 J/(K mol).

A full analysis and computation of heat capacities for the ATHAS data bank involves, then, the following steps: The experimental heat capacities are, naturally, measured at constant pressure, i.e. are C_p, while Eqs. (2-8) yield the heat capacity at constant volume, C_v. Their conversion is accomplished using standard thermodynamic relationships or, if compressibility and expansivity, needed for the conversion are not available, the Nernst-Lindemann approximation [24]:

$$C_p - C_v = 3RA_0C_pT/T_m^\circ \tag{9}$$

with T_m[°] representing the equilibrium melting temperature, and A₀ = 3.9×10⁻³ (K mol)/J, an approximately universal constant. The total experimental C_v is then separated into the part due to the group vibrations and the part due to the skeletal vibrations:

$$C_{v(\text{total})} = C_{v(\text{skeletal})} + C_{v(\text{group vibrations})} \tag{10}$$

The heat capacity due to the group vibrations is calculated from an approximate spectrum obtained independently, as discussed with help of Fig. 4 for polyethylene, and listed for polyoxymethylene [(CH₂-O-)_x] in Table I [25]. The group vibrations of polyethylene can also be taken from Table I since their frequencies (as group vibrations) are changed only little by introducing the ether oxygen. To increase the precision, some of the group vibrations that spread over a wider frequency ranges are approximated by box-distributions. The heat capacity contribution is computed with the help of two one-dimensional Debye functions [16,17] of Eq. (3):

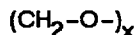
$$C_{v(\text{box})} = NR[\Theta_U/(\Theta_U - \Theta_L)][D_1(\Theta_U/T) - (\Theta_U/\Theta_L)D_1(\Theta_L/T)] \tag{11}$$

The lower frequency limit is given by Θ_L, the upper one by Θ_U. Subtraction of all heat capacity contributions of the group vibrations from the measured C_v yields the experimental, skeletal heat capacity contribution [Eq. (10)].

Table I

The last step in the ATHAS analysis is to assess the skeletal heat capacity. The skeletal vibrations are coupled in such a way that their distribution stretches to zero frequency (i.e. to the acoustical vibrations). In the lowest frequency region one must, in addition, consider that the vibrations will couple intermolecularly. The wavelengths of the vibrations become larger than the molecular anisotropy of the chain structure. As a result, the detailed molecular arrangement is of little consequence at these frequencies. A three-dimensional Debye function as written in Eqs. (7 and 8) should apply. Only above this frequency range does the linearity of the molecules suggest a

Approximate Vibrational Spectrum of Polyoxymethylene



Skeletal Vibrations:

$$N = 2; \theta_1 = 232 \text{ K}; \theta_3 = 117 \text{ K};$$

Group Vibrations:

Vibration Type	Θ _E , Θ _L , Θ _U (K)	N
CH ₂ symm. stretch	4284.7	1.00
CH ₂ asym. stretch	4158.2	1.00
CH ₂ bending	2104.5	1.00
CH ₂ wagging	2018.6	1.00
CH ₂ twisting	1921.9	1.00
CH ₂ rocking	1524.7	0.20
	1707.2	0.24
	1524.7-1707.2	0.56
C-O stretching	1385.1	0.22
	1682.1	0.11
	1385.1-1682.1	0.87
	1304.6	1.00
chain bending	869.7	1.00
	555.0	0.23
	359.7-440.2	0.28
	359.7-655.0	0.48

constant number of vibrations for each frequency (as was also observed in Fig. 2). To approximate all skeletal vibrations of linear macromolecules, one should thus start out at low frequency with a three-dimensional Debye function and then switch to a one-dimensional Debye function. Such an approach was derived by Tarasov [26]. The skeletal vibration frequencies are, thus, separated into two groups, the intermolecular group between zero and ν₃, (characterized by a three-dimensional Θ-temperature, Θ₃), and an intramolecular group between ν₃ and ν₁ (characterized by a one-dimensional Θ-temperature, Θ₁):

$$C_{v(\text{Tarasov})} = NR\{D_1(\Theta_1/T) - (\Theta_3/\Theta_1)[D_1(\Theta_3/T) - D_3(\Theta_3/T)]\} \tag{12}$$

Equation (12) suggests the needed computations and reveals that by assuming that the fraction of vibrators in the intermolecular part is θ_3/θ_1 , one has only two adjustable parameters. The approximate frequency distribution is thus fitted to the experimental skeletal C_p at low temperatures to get θ_3 (0 to θ_3 K) and at higher temperatures, to get θ_1 (θ_3 to θ_1 K). More precise computer programs that accomplish the fitting over the whole temperature region are available [27]. Recently neural network computations have been used for the evaluation of the θ -temperatures [28]. For crystalline polyethylene the best fit was obtained for the θ_1 -temperature of 519 K, and the θ_3 -temperature of 158 K. The data for polyoxymethylene are listed in Table I. These frequencies are close to the end of the ν^2 -dependence of the actual frequency spectrum [25].

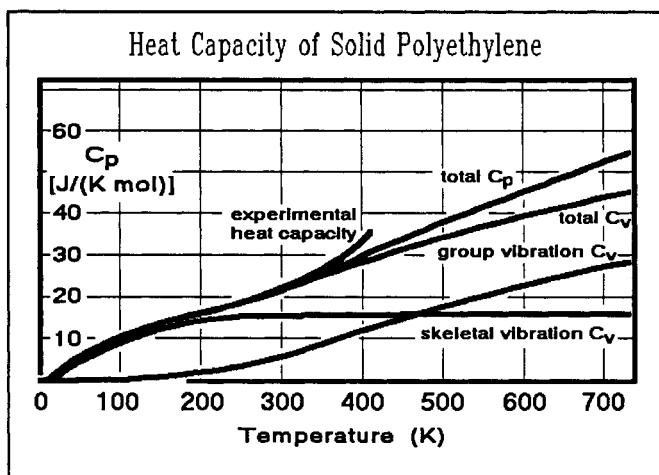


FIGURE 5

References to detailed discussions of the approximate spectra fitted to experimental heat capacities for over 100 polymers are given in the *ATHAS* data bank. Attempts to increase the precision of the description by separating the bending and torsional modes of Fig. 4 with separate θ -temperatures leads to more complicated fitting routines without significant increase in the quality of the description [14]. With the table of group vibration frequencies, the two θ -temperatures and the number of skeletal vibrators, N , it is now possible, in turn, to calculate C_v , and with help of Eq. (9) also C_p . The computations cover now the whole temperature range and are fitted to the experiment only at two temperatures.

Figure 5 shows such calculation for polyethylene. The contribution of the skeletal and group vibrations are shown separately. Deviations starting at about 300 K are linked to conformational motion and disorder that could be studied by molecular dynamics simulations [29].

Since group vibrations are not much affected by changes in their chemical environment, it is possible from the data of Table I not only to compute C_p of polyoxymethylene, but also of all other aliphatic polyoxides.

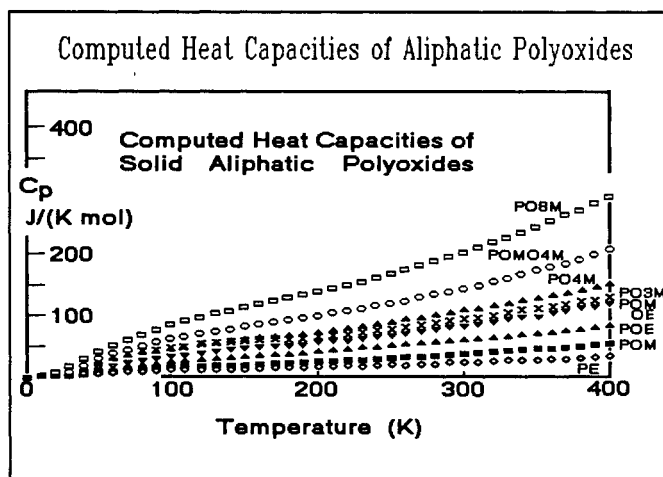


FIGURE 6

Figure 6 shows the results for a series of polyoxides for which some experimental data are available in the *ATHAS* data bank. The abbreviations are to be translated as follows:

PO8M	=	Polyoxyoctamethylene $[O-(CH_2)_8]_x$
POMO4M	=	Polyoxymethyleneoxytetramethylene $[O-CH_2-O-(CH_2)_4]_x$
PO4M	=	Polyoxytetramethylene $[O-(CH_2)_4]_x$
PO3M	=	Polyoxytrimethylene $[O-(CH_2)_3]_x$
POMOEO	=	Polyoxymethyleneoxyethylene $[O-CH_2-O-(CH_2)_2]_x$
POE	=	Polyoxyethylene $[O-(CH_2)_2]_x$
POM	=	Polyoxymethylene $[O-CH_2]_x$
PE	=	Polyethylene (polymethylene) $[CH_2]_x$

Figure 7 shows furthermore, that the θ_1 and θ_3 values for the polyoxides are continuously changing with chemical composition. It is thus possible to estimate θ_1 and θ_3 for intermediate compositions, and to compute heat capacities of unknown polyoxides or copolymers of different monomers without reference to any measurement.

Similar analyses were done for more than 100 macromolecules. The data for N , θ_1 and θ_3 , together with the ranges of experimental C_p -data as well as full data tables of C_p , H , S , and G , as well as the transition parameters and group vibrations are collected in the *ATHAS* data bank. The precision of these computed heat capacities is for most polymers better than $\pm 5\%$.

The strict additivity of the heat capacity contributions of the group vibrations and the continuous change in θ_1 with chemical composition led to the development of addition schemes for heat capacities. As long as the contributions of the backbone groupings that make up the polymer are known empirically, an estimate of the heat capacity of unknown polymers and copolymers is possible. Detailed tables can be found in Refs. 30 and 31.

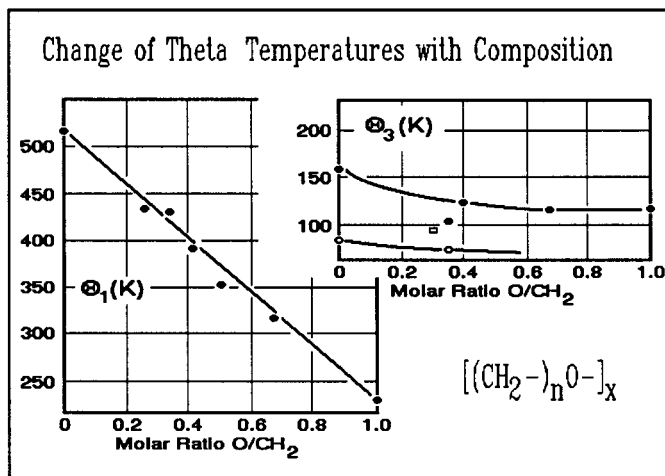


FIGURE 7

Heat Capacity of Liquids

The heat capacities of liquids are much more difficult to understand. The motion involves, besides the vibrations discussed in the last section, also large-amplitude rotations, internal rotations (conformational motion) and translations. Only a first beginning has been made in the more detailed discussion of the heat capacities of liquid macromolecules [18].

Since in the liquid state, polymers are usually in equilibrium, measurements are more reproducible. It was discovered on hand of the large volume of data on liquid macromolecules that addition schemes can help to connect these heat capacities. Figure 8 shows the experimental data for the liquids of the same series of polyoxides as shown in Fig. 6 for the solid state. The equation at the top of the graph represents all the thin lines, the thick lines represent the experimental data [32]. The equation for C_p^a was arrived at by least square fitting of all experiments. Again, the *ATHAS* data bank gives a listing for available data on other polymers. The heat capacities of many macromolecules are thus available through measurement, computation from approximate vibration spectra, or empirical addition schemes.

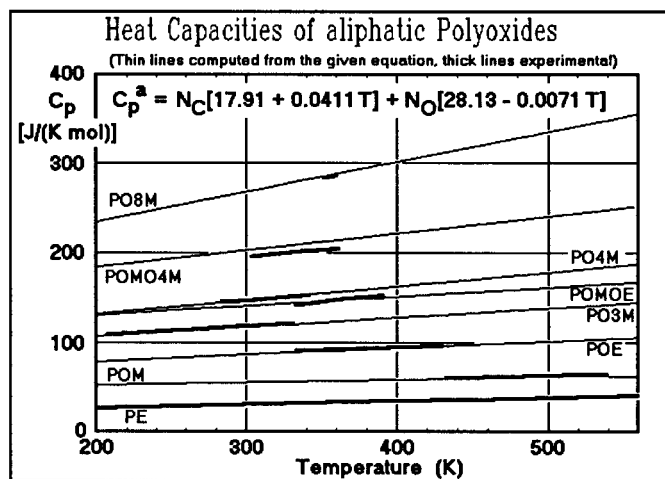


FIGURE 8

Acknowledgements: This work was supported by the Division of Materials Research, the National Science Foundation, Polymers Program, Grant # DMR 90-00520 and the Division of Materials Sciences, Office of Basic Energy Sciences, U.S. Department of Energy, under Contract DE-AC05-84OR21400 with Martin Marietta Energy Systems, Inc.

REFERENCES

1. B. Wunderlich and M. Dole, *J. Polymer Sci.*, **24**, 139 (1957).
2. B. Wunderlich and M. Dole, *J. Polymer Sci.*, **24**, 201 (1957).
3. M. Dole and B. Wunderlich, *Makromol. Chemie*, **34**, 29 (1959); B. Wunderlich, *Polymer*, **5**, 125, 611 (1964).
4. B. Wunderlich, *J. Chem. Phys.*, **37**, 1203, 1207, 2429 (1962).
5. B. Wunderlich and H. Baur, *Adv. Polymer Sci.*, **7**, 151 (1970).
6. B. Wunderlich and L. D. Jones, *J. Macromol. Sci., Phys.*, **B3**, 67 (1969).
7. B. Wunderlich, "Macromolecular Physics; Vol. 1, Crystal Structure, Morphology, Defects; Vol. 2, Crystal Nucleation, Growth, Annealing; Vol. 3, Crystal Melting." Academic Press, New York, NY, 1973, 1976, 1980.
8. B. Wunderlich, *J. Phys. Chem.*, **64**, 1052 (1960).
9. B. Wunderlich, D. M. Bodily, and M. H. Kaplan, *J. Appl. Phys.*, **35**, 95 (1964).
10. A. Weitz and B. Wunderlich, *J. Polymer Sci., Polymer Phys. Ed.*, **12**, 2473 (1974).
11. B. Wunderlich and S. Z. D. Cheng, *Gazz. Chim. Italiana*, **116**, 345 (1986); B. Wunderlich, *Shin Netsu Sokuteino Shinpo*, **1**, 71–100 (1990); M. Varma-Nair, Y. Jin, and B. Wunderlich, in J. Menon, ed. "Trends in Polymer Science." Research Trends, Trivandrum, India, in print, 1994.
12. *ATHAS* data bank, updated every 6 months, please request copy from the author. For the data bank of experimental heat capacities see: U. Gaur, S.-F. Lau, H.-C. Shu, B. B. Wunderlich, M. Varma-Nair, and B. Wunderlich, *J. Phys. Chem. Ref. Data*, **10**, 89, 119, 1001, 1051 (1981); **11**, 313, 1065 (1982); **12**, 29, 65, 91 (1983); and (1990), **20**, 349–404 (1991).
13. H. Suzuki, J. Grebowicz, and B. Wunderlich, *Brit. Polymer J.*, **17**, 1 (1985).
14. B. Wunderlich and J. Grebowicz, *Adv. Polymer Sci.*, **60/61**, 1 (1984).
15. B. Wunderlich, "Thermal Analysis." Academic Press, New York, NY, 1990.
16. P. Debye, *Ann. Physik*, **39**, 789 (1912).
For computer programs and a general discussion of the Debye functions see: Yu. V. Cheban, S. F. Lau and B. Wunderlich, *Colloid Polymer Sci.*, **260**, 9 (1982).
17. For tables of the one-dimensional Debye Function see:
B. Wunderlich, *J. Chem. Phys.*, **37**, 1207 (1962).
18. K. Loufakis and B. Wunderlich, *J. Phys. Chem.*, **92**, 4205 (1988).
19. A. Einstein, *Ann. Physik*, **22**, 180, 800 (1907).
20. Tables of the Einstein Function can be found, for example, in J. Sherman and R. B. Ewell, *J. Phys. Chem.*, **46**, 641 (1942); D. R. Stull and F. D. Mayfield, *Ind. Eng. Chem.*, **35**, 639 (1943); J. Hilsenrath and G. G. Ziegler, "Tables of Einstein Functions," *Natl. Bur. Stands. Monograph*, **49** (1962). By now, any good pocket calculator is, however, able to give 10 digit precision with programmed calculation within a fraction of a second.
21. For tables of the two-dimensional Debye Function see:
U. Gaur, G. Pultz, H. Wiedemeier and B. Wunderlich, *J. Thermal Anal.*, **21**, 309 (1981).
22. For tables of the three-dimensional Debye Function see:
J. A. Beatty, *J. Math. Phys. (MIT)*, **6**, 1 (1926/27).
23. For a discussion of the frequency spectrum of polyethylene see: J. Barnes and B. Fanconi, *J. Phys. Chem. Ref. Data*, **7**, 309 (1978).
24. R. Pan, M. Varma, and B. Wunderlich, *J. Thermal Anal.*, **35**, 955 (1989).
25. J. Grebowicz, H. Suzuki and B. Wunderlich, *Polymer*, **26**, 561 (1985).
26. V. V. Tarasov, *Zh. Fiz. Khim.*, **24**, 111, (1950); **27**, 1430 (1953); see also: *ibid.* **39**, 2077 (1965); *Dokl. Akad. Nauk SSSR*, **100**, 307 (1955).
27. S.-F. Lau and B. Wunderlich, *J. Thermal Anal.*, **28**, 59 (1983).
28. D. W. Noid, M. Varma-Nair, B. Wunderlich, and J. A. Darsey, *J. Thermal Analysis*, **37**, 2295 (1991).
29. D. W. Noid, B. G. Sumpter, M. Varma-Nair, and B. Wunderlich, *Makromolekulare Chemie, Rapid Commun.*, **10**, 377 (1989).
30. U. Gaur, M.-Y. Cao, R. Pan and B. Wunderlich, *J. Thermal Anal.*, **31**, 421 (1986).
31. R. Pan, M.-Y. Cao and B. Wunderlich, *J. Thermal Anal.*, **31**, 1319 (1986).
32. H. Suzuki and B. Wunderlich, *J. Polymer Sci., Polymer Phys. Ed.*, **23**, 1671 (1985).